



1
2
3
4
5
6
7
8
9
10
11
12
13
14
15
16
17
18
19
20
21
22
23
24
25
26
27
28

**Sea ice break-up and freeze-up indicators for users
of the Arctic coastal environment**

John E. Walsh¹, Hajo Eicken¹, Kyle Redilla¹, Mark Johnson²

¹International Arctic Research Center, University of Alaska, Fairbanks AK 99775 USA

²College of Fisheries and Ocean Sciences, University of Alaska, Fairbanks AK 99775 USA

Correspondence to: John E. Walsh (jewalsh@alaska.edu)



29

Abstract

30 Arctic coastal waters are characterized by seasonal retreat and advance of sea ice. The timing
31 of advance and retreat varies substantially from year to year. Various activities, ranging from
32 marine transport to the use of sea ice as a platform for industrial activity or winter travel, are
33 affected by variations in the timing of break-up and freeze-up, resulting in a need for
34 indicators to document the regional and temporal variations in coastal areas. Here we develop
35 indicators based on daily sea ice concentrations derived from satellite passive microwave
36 measurements. The “day of year” indicators are designed to optimize value for users while
37 building on past studies characterizing break-up and freeze-up dates in the open pack ice.
38 Relative to indicators for broader adjacent seas, the coastal indicators show later break-up at
39 sites known to have extensive landfast ice, for which break-up typically lags retreat of the
40 adjacent, thinner drifting ice. The coastal indicators also show an earlier freeze-up at some
41 sites in comparison with freeze-up for broader offshore regions, likely tied to earlier freezing
42 of shallow water regions and areas affected by freshwater input from nearby streams and
43 rivers. A factor analysis performed to synthesize the local indicator variations shows that the
44 local break-up and freeze-up indicators have greater spatial variability than corresponding
45 metrics based on regional ice coverage. However, the trends towards earlier break-up and
46 later freeze-up are unmistakable over the post-1979 period in the synthesized metrics of the
47 coastal break-up/freeze-up and their corresponding regional ice coverage. The findings imply
48 that locally defined indicators can serve as key links between pan-Arctic or global indicators
49 such as sea-ice extent or volume and local uses of sea ice, with the potential to inform
50 community-scale adaptation and response.

51 *Key words:* sea ice, Arctic, break-up, freeze-up, ice concentration



52 1. Introduction

53 Coastal sea ice impacts residents and other users of the offshore environment in various ways.
54 Perhaps most obvious is the fact that non-ice strengthened vessels require ice-free waters for
55 marine transport, which can serve purposes such as resupply of coastal communities, the
56 transport of extracted resources (oil, liquefied natural gas, mined metals), migration of marine
57 mammals (e.g., bowhead whales) and wintertime travel over the ice by coastal residents. Key
58 metrics for offshore uses such as these are the timing of break-up (or ice retreat) in the spring
59 and the timing of freeze-up (or ice advance) in the autumn or early winter.

60 Sea ice concentration is the basis of most metrics of the timing (dates) of sea ice break-up and
61 freeze-up (Markus et al., 2009; Johnson and Eicken, 2016; Bliss and Anderson, 2018; Peng et
62 al., 2018; Bliss et al., 2019; Smith and Jahn, 2019). An emerging tendency in these studies is
63 the definition of break-up date as the date on which ice concentration drops below a
64 prescribed threshold and remains below that threshold for a prescribed minimum duration
65 (chosen to eliminate repeated crossings of the concentration threshold as a result of
66 temperature- or wind-driven changes in ice coverage associated with transient weather
67 events). A corresponding criterion is used for the freeze-up date.

68 Coastal regions present special challenges in the application of such criteria. First, shorefast
69 or landfast ice (stationary sea ice held in place along the shoreline through as a result of
70 grounding and/or confinement by the coast) is common in waters immediately offshore of the
71 coast, especially in areas with shallow water. Shorefast ice provides especially important sea
72 ice services because it offers a stable platform for offshore travel, serves as a critical habitat
73 for marine mammals such as seals and polar bears (Dammann et al., 2018), and provides a
74 buffer against coastal storms (Hosekova et al., 2021). Second, sea ice concentrations derived



75 from passive microwave measurements are prone to contamination by microwave emissions
76 from land in coastal grid cells. Finally, many parts of the Arctic coastline have inlets, river
77 deltas and barrier islands that are not captured by the 25 km resolution of the passive
78 microwave product.

79 A key aim of the current study is to contribute to efforts at the national and global scale to
80 establish key sets of indicators that support sustained assessment of climate change and
81 inform planning and decision-making for adaptation action (Kenney et al., 2016; IPCC, 2022).
82 Both at the pan-Arctic and global, as well as the U.S. national level, indicators associated with
83 the state of the sea ice cover so far have focused on the summer minimum and winter
84 maximum extent and ice thickness (AMAP, 2017; Box et al., 2019; IPCC, 2022). As outlined
85 by Box et al. (2019), this approach has been motivated by the objective of describing and
86 tracking the state of key components of the global climate system. However, large-scale (pan-
87 Arctic) measures of e.g., sea-ice extent or volume are of little value and relevance to those
88 needing to adapt or respond to such change at the community or regional scale. Here, we
89 examine the timing of sea-ice freeze-up and break-up as key constraints for a range of human
90 activities and ecosystem functions in Arctic settings.

91 **2. Data and methods**

92 The primary data source used here is the archive of gridded daily sea ice concentrations
93 derived from the SMMR, SSM/I and SSMIS sensors onboard the Nimbus-7 and various
94 DMSP satellites dating back to November, 1978. The dataset, NSIDC-0051 of the National
95 Snow and Ice Data Center (NSIDC), is the NOAA/NSIDC Climate Data Record of Passive
96 Microwave Sea Ice Concentration Version 3. In the construction of this dataset, the NASA
97 Team algorithm (Cavalieri et al., 1984) and the NASA Bootstrap algorithm (Comiso et al.,



98 1986) were used to process the microwave brightness temperatures into a consistent time
99 series of daily sea ice concentrations. The data are on a polar stereographic grid projection
100 with a grid cell size of 25 km x 25 km.

101 The daily sea ice concentrations are used to define the metrics of the start and end of break-up
102 and freeze-up in each year of a 40-year period, 1979-2018. The definitions build on those
103 used by Johnson and Eicken (2016), which were informed by Indigenous experts'
104 observations of ice use and ice hazards in coastal Alaska, and relate to planning and decision-
105 making at the community-scale (Eicken et al., 2014). Here, we expand the satellite data
106 analysis with minor modifications of the break-up and freeze-up criteria to broaden the
107 applicability to non-coastal areas. Examples include imposing maximum and minimum
108 values for the thresholds computed from summary statistics of the daily sea ice concentration
109 values of relevant periods. The revised definitions are presented in Table 1. Prior to applying
110 these definitions, the data were processed with a linear interpolation to fill in missing daily
111 values, followed by a spatial and then temporal smoothing to smooth out short (< 3 days)
112 events.

113 A key objective of this work is to compare the various dates at nearshore locations with
114 the corresponding metrics for broader areas of the Arctic Ocean and the subarctic seas. A set
115 of ten locations was selected on the basis of their geographical distribution and the relevance
116 of local sea ice to uses by communities, industry, military or other stakeholders. These
117 locations are listed in Table 2, together with their geographic coordinates. For each of these
118 locations, several passive microwave grid cells close to (but not adjacent to) the coastline
119 were selected for calculation of the break-up and freeze-up metrics. Figure 1 shows
120 geographical insets illustrating the proximity of the selected grid cells to the coastline.



121 Table 1. Definition of the start and end of break-up and freeze-up.

122	Break-up start	The date of the last day for which the previous two weeks' ice concentration
123		always exceeds a threshold computed as the maximum of (a) the winter
124		(January-February) average minus two standard deviations and (b) 15%.
125		Undefined if the average summer sea ice concentration (SIC) is greater than
126		40% or if the subsequent break-up end is not defined.
127	Break-up end	The first date after the break-up start date for which the following two weeks'
128		ice concentration is less than a threshold computed as the maximum of (a)
129		the summer (August-September) average plus one standard deviation and (b)
130		50%. Undefined if the daily SIC is less than the threshold for the entire
131		summer or if break-up start is not defined.
132	Freeze-up start:	The date on which the ice concentration exceeds for the first time a threshold
133		computed as the maximum of (a) the summer (August-September) average
134		plus one standard deviation and (b) 15%. Undefined if the daily SIC never
135		exceeds this threshold, if the mean summer SIC is greater than 25%, or if
136		subsequent freeze-up end is not defined.
137	Freeze-up end:	The first date after the freeze-up start date for which the following two
138		weeks' ice concentration exceeds a threshold computed as the maximum of
139		(a) the average winter (January-February) ice concentration minus 10% and
140		(b) 15%, and the minimum of this result and (c) 50%. Undefined if daily SIC
141		exceeds this threshold for every day of the search period or if freeze-up start
142		is not defined.

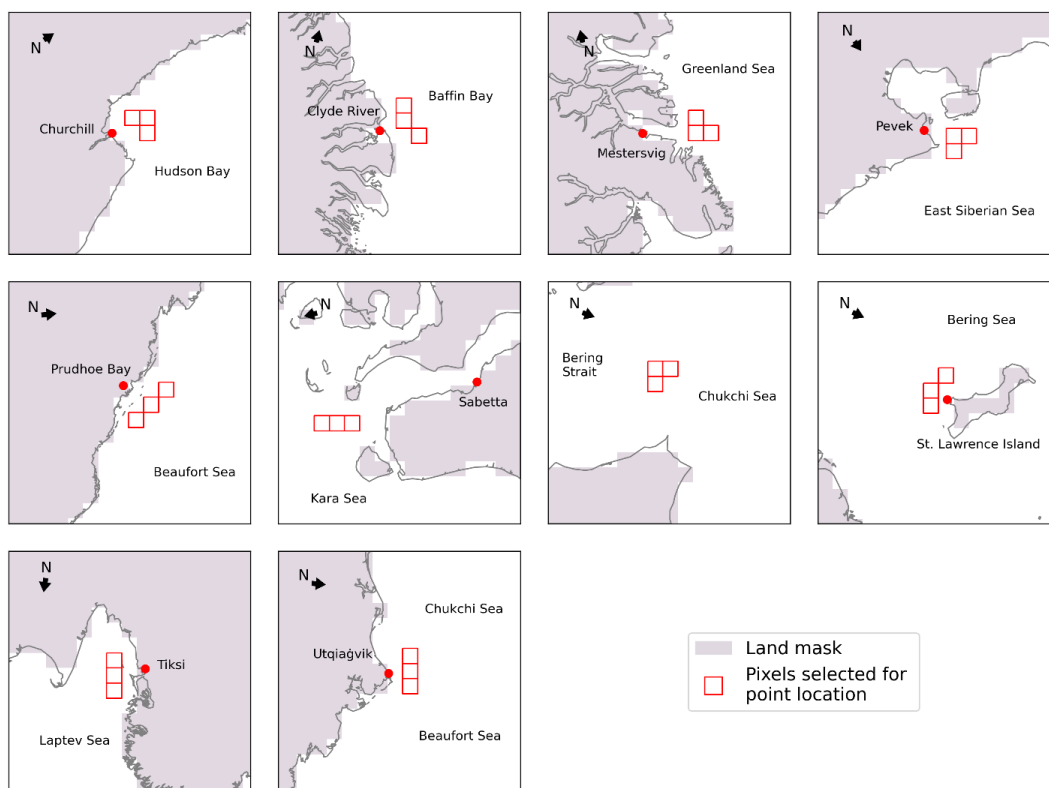


143

144 Table 2. Near-coastal locations selected for calculation of break-up and freeze-up metrics

145	<u>Sea</u>	<u>Location</u>	<u>Latitude, Longitude</u>	<u>Significance of location</u>
146	Beaufort Sea	Prudhoe Bay	70.2N, 148.2W	oil facilities
147	Chukchi/Beaufort Seas	Utqiagvik	71,3N, 156.8W	Indigenous community
148	Chukchi Sea	Bering Strait coast	69.6N, 170W	shipping route
149	Bering Sea	St. Lawrence Island	65.7N, 168.4W	Indigenous community
150	East Siberian Sea	Pevek	69.8N, 170.6E	port, mining facility
151	Laptev Sea	Tiksi	71.7N, 72.1E	research site, port
152	Kara Sea	Sabetta	71.3N, 72.1E	port, LNG facility
153	Greenland Sea	Mestersvig	72.2N, 23.9W	military base
154	Baffin Bay	Clyde River	70.3N, 68.3W	Indigenou community
155	Hudson Bay	Churchill	58.8N, 94.2W	port, tourism

156



157

158 Figure 1. Grid cells used for sea ice indicator metrics corresponding to coastal locations (red
159 dots).

160 Previous studies cited earlier have evaluated break-up and freeze-up metrics for subregions of
161 the Arctic Ocean and the surrounding seas. For comparisons with similar regions, we utilize
162 the MASIE (Multisensor Analyzed Sea Ice Extent) regionalization
163 (https://nsidc.org/data/masie/browse_regions). Of the MASIE regions shown in Figure 1, we
164 choose the following for computation of regionally averaged metrics of break-up and freeze-
165 up: (1) Beaufort Sea, (2) Chukchi Sea, (3) East Siberian Sea, (4) Laptev Sea, (5) Kara Sea, (6)
166 Barents Sea, (7) Greenland Sea, (8) Baffin Bay, (9) Canadian Archipelago, (10) Hudson Bay,
167 (11) Central Arctic and (12) Bering Sea.



168



169

170 Figure 2. The MASIE subregions of the Arctic. Regions utilized in this study (see Table 2)
171 include #s 1 (Beaufort Sea), 2 (Chukchi Sea), 3 (East Siberian Sea), 4 (Laptev Sea), 5 (Kara
172 Sea), 7 (Greenland Sea), 8 (Baffin Bay), 10 (Hudson Bay) and 12 (Bering Sea).

173

174 The following section includes time series of the local indicators and, for comparison,
175 time series of the corresponding regional indicators. In order to address the spatial coherence
176 of the indicators, we performed a factor analysis on the different sets (break-up/freeze-up,
177 start/end dates) of ten regional indicators. Factor analysis is a statistical method for



178 quantifying relationships among a set of variables. The variability in the overall dataset is
179 depicted by a set of factors. Each factor explains a percentage of the total variance in space
180 and time. Each variable in each factor is given a loading (or weight) based on its contribution
181 to the variance explained by that factor. The first factor can be viewed as the linear
182 combination of the variables that maximizes the explained variance in the overall dataset. The
183 second and each successive factor maximizes the variance unexplained by the preceding
184 factors. Successive factors explain successively smaller fractions of the overall variance.
185 Multiple variables can have strong loadings in the same factor, indicating they follow a
186 similar pattern and are likely highly related. Factor analysis has a long history of applications
187 to Arctic sea ice variability (Walsh and Johnson, 1982; Fang and Wallace, 1994; Deser et al.,
188 2000; Fu et al., 2021). The factor analysis calculations used here were performed using the
189 XLSAT software package run in Excel (<https://www.xlstat.com/en/>)

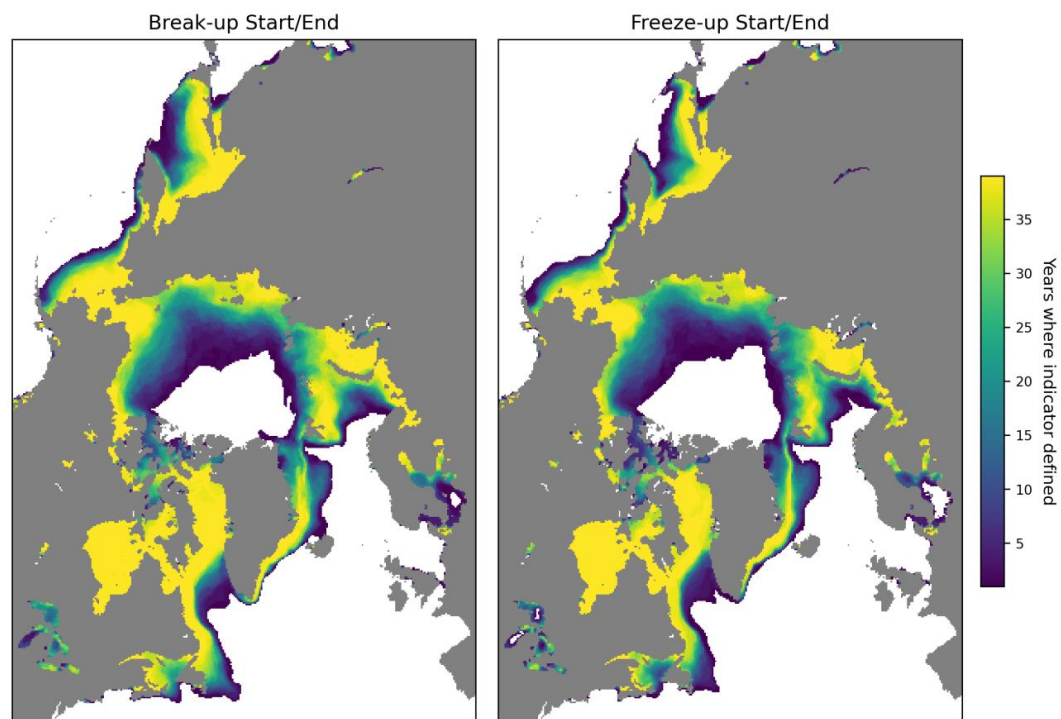
190 **3. Results**

191 With coastal ice retreat and onset of ice advance as this study's primary focus, we first
192 demonstrate the applicability of the indicators evaluated here. The various metrics of sea ice
193 break-up and freeze-up in Table 2 are not defined for all locations in the Arctic. For example,
194 locations that remain ice-covered throughout a particular year will not be assigned dates for
195 any of the indicators in that year, and the same is true of locations at which sea ice does not
196 form during a particular year. Figure 3 shows the number of years in the 1979-2018 study
197 period during which the break-up and freeze-up indicators are actually defined. It is apparent
198 that the indicators are consistently defined in the seasonal sea ice zone spanning the subarctic
199 seas. In particular, all ten coastal locations in Table 2 are in the yellow areas (>35 years out of
200 40 years defined) of Figure 3. Of note in Figure 3 is that the number of years with defined



201 break-up indicators slightly exceeds (by one) the number of years with freeze-up indicators at
202 some locations at the outer periphery of the seasonal sea ice zone. These are locations in
203 which sea ice was present for some portion of the early years but not at the end of the study
204 period, so in one of the years there was a break-up but no freeze-up.

205



206

207 Figure 3. Number of years in the 1979-2018 study period in which the break-up and freeze-up
208 indicators were defined.

209

210



211 A key issue to be addressed is the degree to which the indicators utilized here differ from
212 those of previous studies. The metrics of Bliss et al. (2019) or similar variants have been used
213 in recent publications and provide natural points of comparison. While there are various
214 differences between our metrics and those of Bliss et al., the most consequential for the
215 computed dates is the use of departures from winter/summer averages concentrations in our
216 criteria vs. Bliss et al.'s use of 15% and 80% concentrations as key thresholds.

217 The four indicators in this study are the dates of the start and end of break-up and freeze-up.
218 The corresponding indicators used by Bliss et al. (2019) are the date of opening (defined as
219 the last day on which the ice concentration drops below 80% before the summer minimum),
220 the date of retreat (defined as the last day the ice concentration drops below 15% before the
221 summer minimum), the date of advance (defined as the first day the ice concentration
222 increases above 15% following the final summer minimum) and the date of closing (defined
223 as the first day the ice concentration increases above 80% following the final summer
224 minimum). Figure 4 shows that there are systematic differences between our metrics (based
225 on Johnson and Eicken, 2016; hereafter denoted as J&E) and those of Bliss et al. when the
226 two sets of metrics are evaluated for the MASIE regions. In particular, J&E's start and end of
227 breakup generally occur earlier by up to several weeks than the corresponding dates of
228 opening and retreat defined by Bliss et al. On the other hand, J&E's freeze-up dates are more
229 closely aligned with those of Bliss et al., although J&E's end-of-freeze-up occurs later (by 1
230 to 3 weeks) than Bliss et al.'s closing date in most of the MASIE regions, especially the North
231 Atlantic and Canadian regions.

232 The violin plots in Figure 4 show distributions but not the temporal variations that have been
233 indicated by results of previous studies (Peng et al., 2018; Bliss et al., 2019). Figures 5 and 6

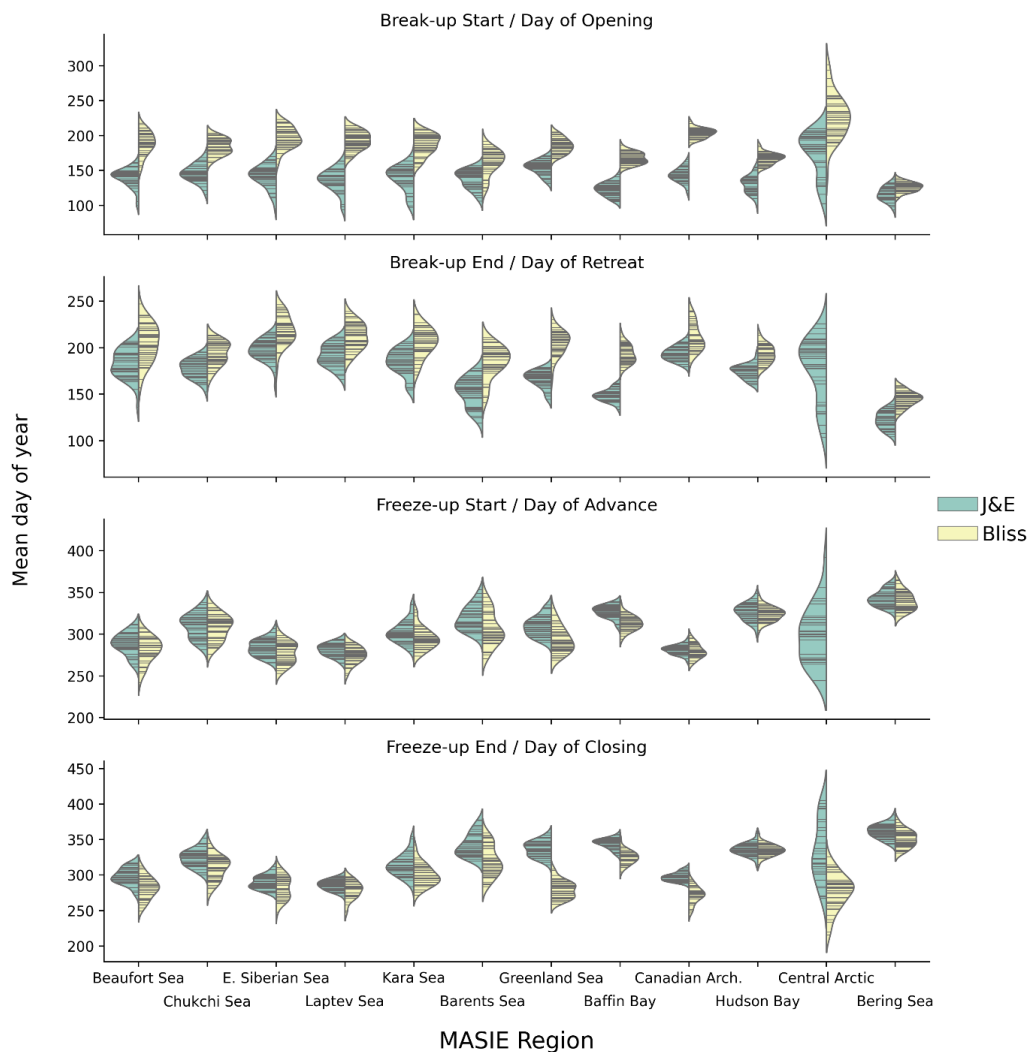


234 provide the temporal perspective on the end dates of break-up (Day of retreat) and freeze-up
235 (Day of closing), respectively. In each of the MASIE regions, the J&E criterion gives an
236 earlier break-up date. The difference is typically two to three weeks, although it exceeds a
237 month in the Greenland Sea and Baffin Bay. Despite the offsets, the trends are nearly the
238 same in nearly all the regions. Exceptions are the Canadian Archipelago, where the J&E trend
239 is weaker than the Bliss trend, and the Bering Sea, where the trends are opposite in sign.
240 However, the trend in the Bering region is not statistically significant at the 99% level by
241 either metric, in contrast to all other regions in which the trends are significant at this level.
242 The main conclusion from Figure 5 is that, except for the Bering Sea, sea ice break-up is
243 occurring earlier throughout the Arctic than several decades ago, no matter which metric is
244 used.

245 In contrast to the trends towards earlier breakup, the J&E and Bliss metrics for the end of
246 freeze-up both show significant trends towards later dates in most of the MASIE regions
247 (Figure 6). In this case, even the Bering Sea shows a trend towards later freeze-up. Again,
248 there is an offset towards a later date with the J&E metric, although the offset has a range
249 among the region, from essentially zero in Hudson Bay to more than six weeks in the
250 Greenland Sea. The trends, however, show less agreement in some regions than do the trends
251 for break-up dates in Figure 5. The J&E trends are more strongly positive in the seas of the
252 eastern Russian sector: the Chukchi, East Siberian and Laptev Seas. The same is true,
253 although to a lesser degree, in the Barents Sea and the Canadian Archipelago. The main
254 message from Figure 6 is that the freeze-up is ending later throughout the Arctic, although the
255 magnitude of the trend is more sensitive to the criteria used for end-of-freeze-up than for end-
256 of-break-up.



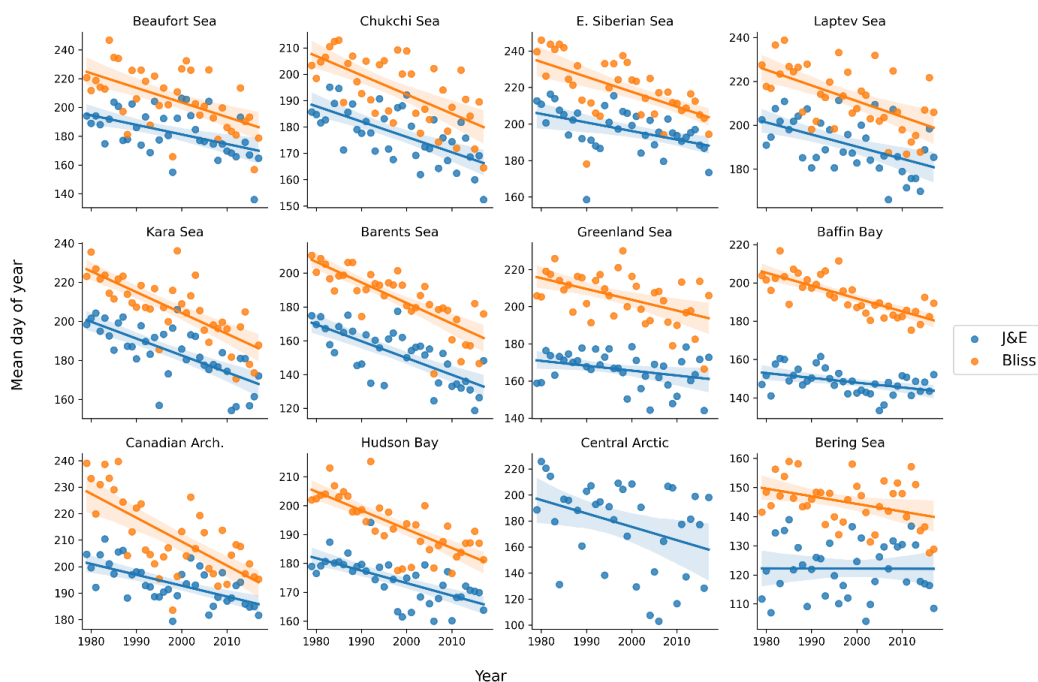
257



258

259 Figure 4. Violin plots of the Julian dates of the break-up/freezing metrics used in this study
260 based on Johnson and Eicken (2016) (green shading) and the corresponding dates of ice
261 opening, retreat, advance and closing as defined by Bliss et al. (2019).

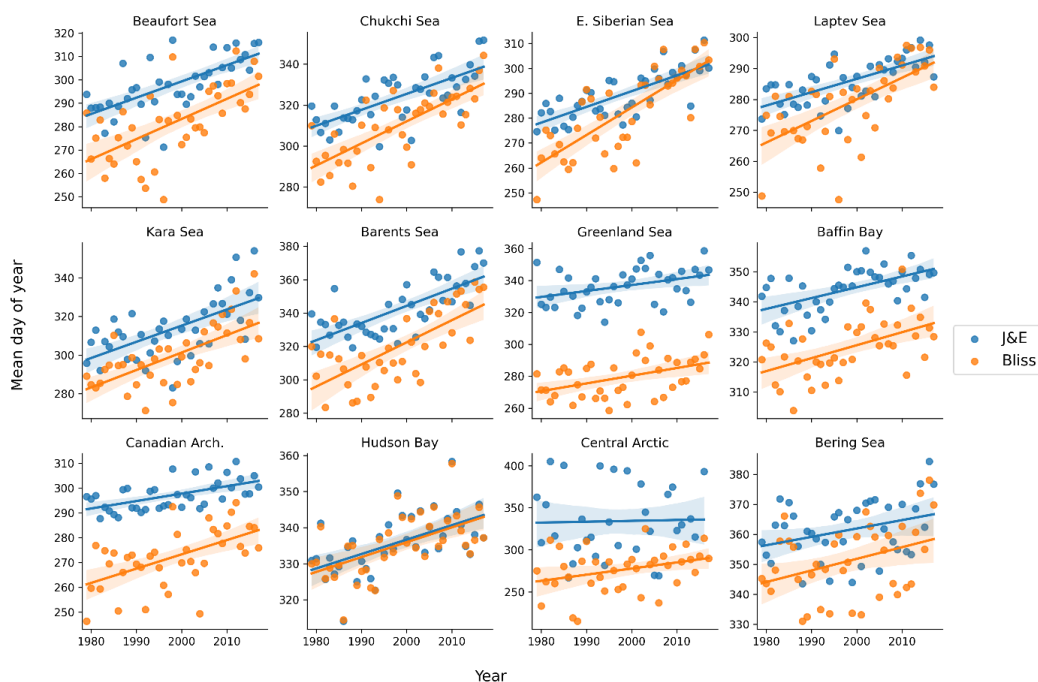
262



263

264 Figure 5. Yearly values of J&E’s break-up end date (blue symbols) and the Bliss et al.’s
265 (2019) Day of retreat (orange symbols) in the various MASIE regions. Corresponding trend
266 lines are shown in each panel. (For the Central Arctic region, the Bliss metric (Day of retreat)
267 was not defined for a sufficient number of years).

268



269

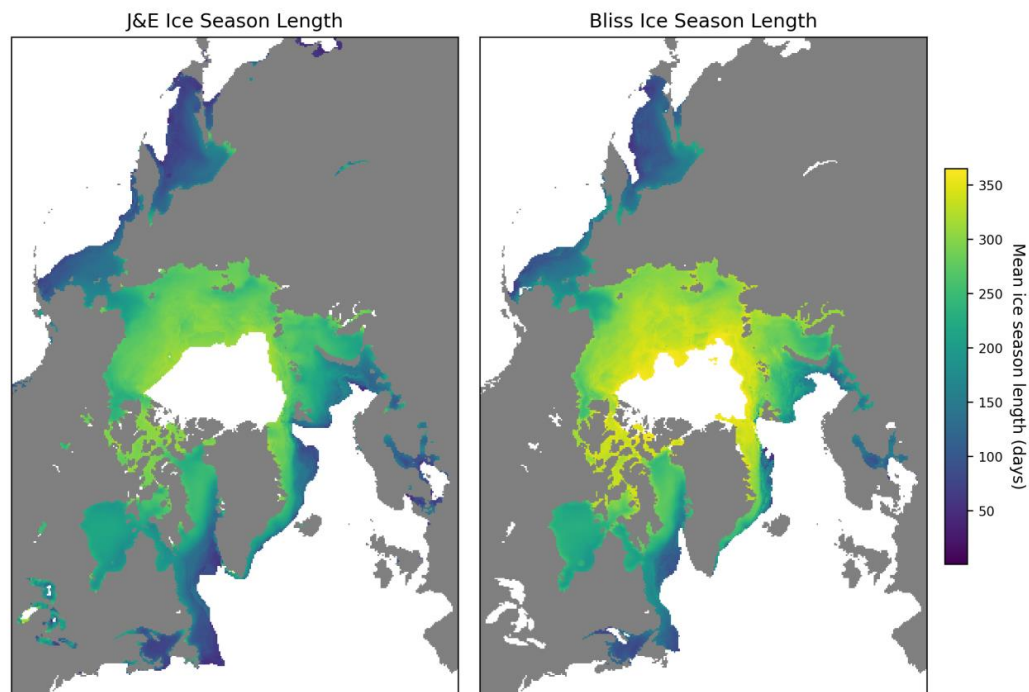
270 Figure 6. Yearly values of J&E’s freeze-up end date (blue symbols) and the Bliss et al.’s
271 (2019) Day of closing (orange symbols) in the various MASIE regions. Corresponding trend
272 lines are shown in each panel. Y-axes labels are Julian dates.

273

274 A final comparison is presented in Figure 7, which shows the ice season lengths computed
275 using the two sets of metrics. The ice season length is defined as the number of days between
276 the end of freeze-up and the start of break-up. Consistent with J&E’s earlier break-up (Figure
277 5) and later freeze-up (Figure 6), the ice season length is generally longer when computed
278 from the J&E metrics. The differences in Figure 7 exceed a month in most of the Arctic
279 except for the Bering Sea, Hudson Bay and the Canadian Archipelago. However, the negative
280 trends of ice season length are similar in magnitude according to both sets of metrics over



281 most of the Arctic. The trend maps are not shown here because they add little to the
282 information conveyed in Figures 5 and 6.



283

284 Figure 7. Mean ice season length based on the J&E metrics (left) and the Bliss et al. (2019)
285 metrics (right). Metrics of break-up and freeze-up were not defined in a sufficient number of
286 years in the white area near the North Pole.

287

288 The main focus of the present study is the relationship between the indicators for the coastal
289 locations and those for the broader MASIE regions containing the coastal locations. Figures
290 8-11 provide these comparisons for all four metrics defined by the modified J&E algorithms.
291 In all cases, the yearly values (and linear trend lines) for the ten coastal locations in Table 2



292 are plotted for the 1979-2018 period, together with the values for the corresponding MASIE
293 regions.

294 The break-up start dates (Figure 8) differ between the coastal locations and the broader
295 MASIE regions in most of the ten cases, and in some cases the trends are notably different.
296 With regard to systematic differences, not only the magnitude but also the sign of the offsets
297 varies among the regions. The break-up start date at the coast is later than for the MASIE
298 regions for Prudhoe (Beaufort Sea), Utqiagvik (Chukchi Sea), Tiksi (Laptev Sea), and both
299 Canadian locations: Churchill (Hudson Bay) and Clyde River (Baffin Bay). These sites are all
300 Arctic coastal locations at which varying extents of landfast ice are present. By contrast, the
301 coastal locations have earlier break-up start dates (relative to their corresponding MASIE
302 regions) at St. Lawrence Island (Bering Sea), Mestersvig (Greenland Sea) and the Bering
303 Strait (Chukchi Sea). These locations are less prone to experience a buildup of landfast ice
304 during the winter. The results imply that landfast ice is a key determinant of the timing of the
305 start of breakup relative at coastal locations relative to the broader sector of the seasonal sea
306 ice zone.

307 While the general trend towards earlier break-up noted above (Figure 5) is apparent at most of
308 the coastal locations, the magnitudes of the trends can differ between the coastal sites and the
309 broader MASIE regions. Figure 8 shows that, in most cases, the trend towards an earlier start
310 of break-up is stronger at the coastal location relative to the MASIE region at Churchill, Clyde
311 River, Pevek and Sabetta. Only at Tiksi is the negative trend weaker at the coastal site. In the
312 other regions the trends are nearly identical.

313 The break-up end dates (Figure 9) show differences similar to those in Figure 8 in most, but
314 not all, cases. The break-up end date occurs earlier at Clyde River, Prudhoe and Utqiagvik

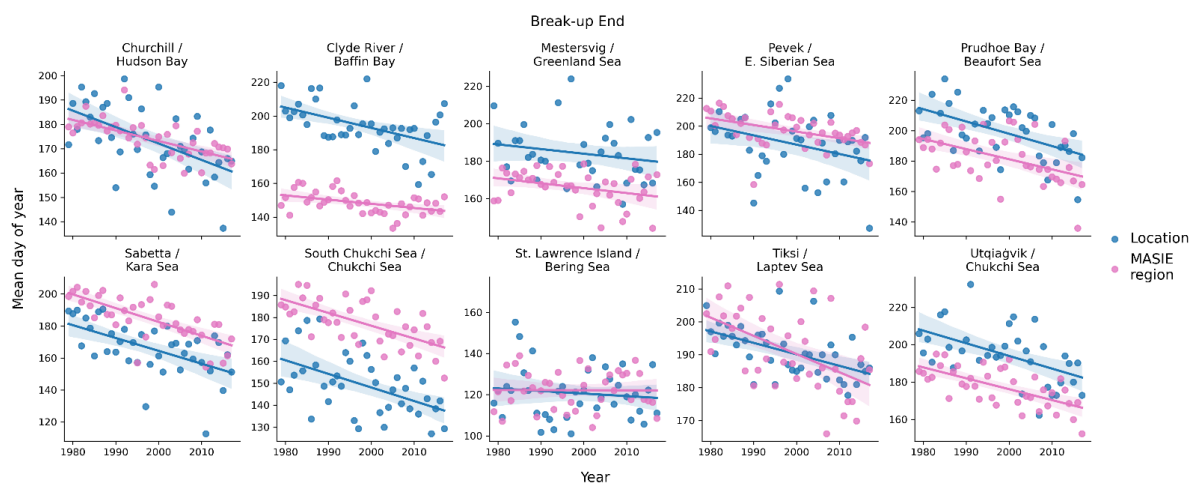


315 relative to the MASIE regions, as is the case with the results in Figure 8. However, unlike the
316 break-up start date, the break-up end date also occurs earlier at Mestersvig than for the
317 Greenland Sea MASIE region. The opposite relationship is found in the Kara Sea (Sabetta)
318 and the South Chukchi Sea (Bering Strait), where the MASIE region has the earlier break-up
319 end date. The temporal trends in the break-up end dates are generally similar for the coastal
320 locations and the MASIE regions, and there are no differences in sign. All coastal locations
321 and all MASIE regions show negative trends, i.e., trends toward earlier break-up end dates in
322 recent decades.



323

324 Figure 8. Yearly values (1979-2018) of the break-up start dates for the coastal locations
325 (blue) and the corresponding MASIE regions (purple). Linear regression lines are shown with
326 the same color coding. In each panel, the upper line of header identifies the coastal location
327 and the lower line identifies the MASIE region. All values are based on the modified J&E
328 algorithms.



329

330

Figure 9. Same as Figure 8, but for the break-up end dates.

331

332 The freeze-up start dates are compared in Figure 10. Several regions show large offsets, most
333 notably Clyde River (Baffin Bay) and Mestersvig (Greenland Sea), where the start of freeze-
334 up occurs earlier at the coast by several weeks. Both Baffin Bay and the Greenland Sea are
335 large MASIE regions (Figure 2), favoring the delay of freeze-up over a substantial portion of
336 the seasonal sea ice zone within the respective MASIE regions. Freeze-up dates are also
337 earlier than offshore at several other coastal locations: Churchill, Sabetta and Utqiagvik.
338 These are regions in which it is common for ice to form along the coast in autumn, with the
339 ice edge advancing offshore to meet the expanding main ice pack as freeze-up progresses. By
340 contrast, the southern Chukchi Sea location has a later freeze-up date than the Chukchi
341 MASIE region, largely because the southern Chukchi grid cells are located in an area of
342 relatively warm inflowing currents and are in the southern portion of the Chukchi MASIE

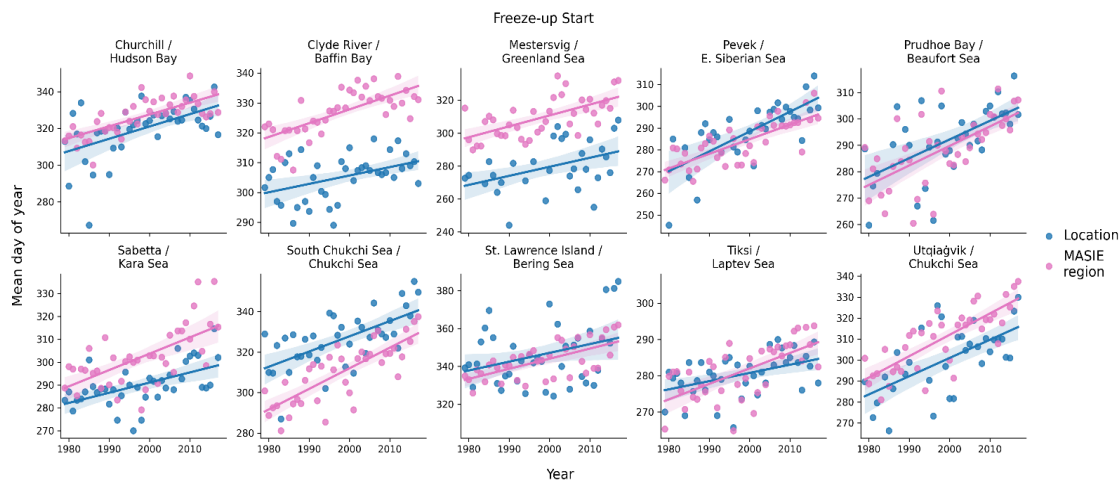


343 region. As with the break-up end dates, all coastal locations and MASIE regions show trends
344 of the same sign. In this case, the trends are all positive, indicating a later start to freeze-up.

345 Finally, Figure 11 compares the freeze-up end dates for the ten coastal sites and their MASIE
346 regions. The results are quite similar to those for the freeze-up start dates in Figure 10.

347 Relative to the MASIE regions as a whole, freeze-up ends earlier at both Canadian sites
348 (Churchill and Clyde River), Mestersvig, Sabetta and Utqiaġvik. Again, the differences are
349 especially large (more than a month) at Clyde River and Mestersvig, both of which are in
350 large MASIE regions as noted above. The southern Chukchi Sea and, to a lesser extent in
351 recent decades, Pevek (East Siberian Sea) show later freeze-ups near the coast than for the
352 MASIE region. Once again, all trends are positive, pointing to a later end to freeze-up at
353 coastal as well as offshore regions throughout the Arctic. The changes in the freeze-up dates
354 over the 40-year period are especially large, exceeding one month, at Pevek (East Siberian
355 Sea) and Prudhoe (Beaufort Sea). The changes are close to a month at Utqiaġvik (Chukchi
356 Sea) and the Southern Chukchi Sea.

357

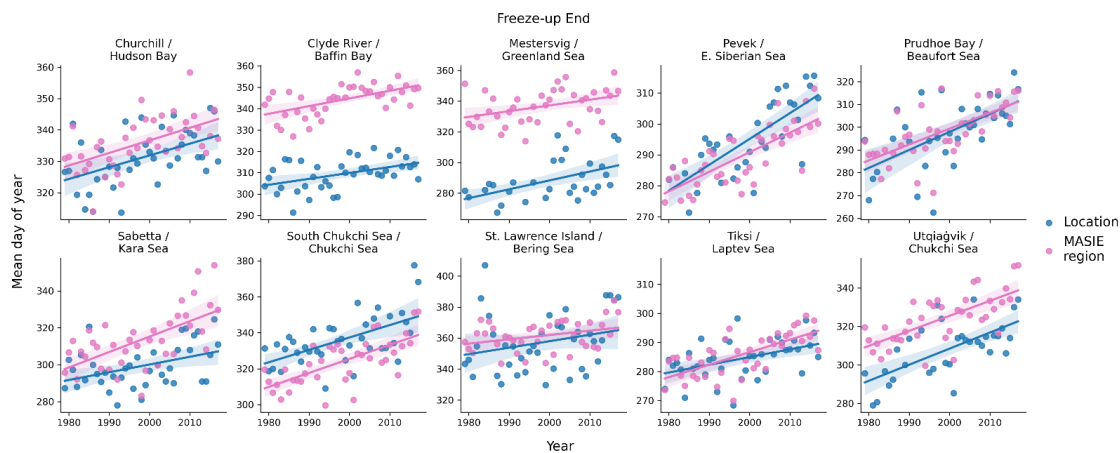


358

359

Figure 10. Same as Figure 8, but for the freeze-up start dates.

360



361

362

Figure 11. Same as Figure 8, but for the freeze-up end dates.

363

364



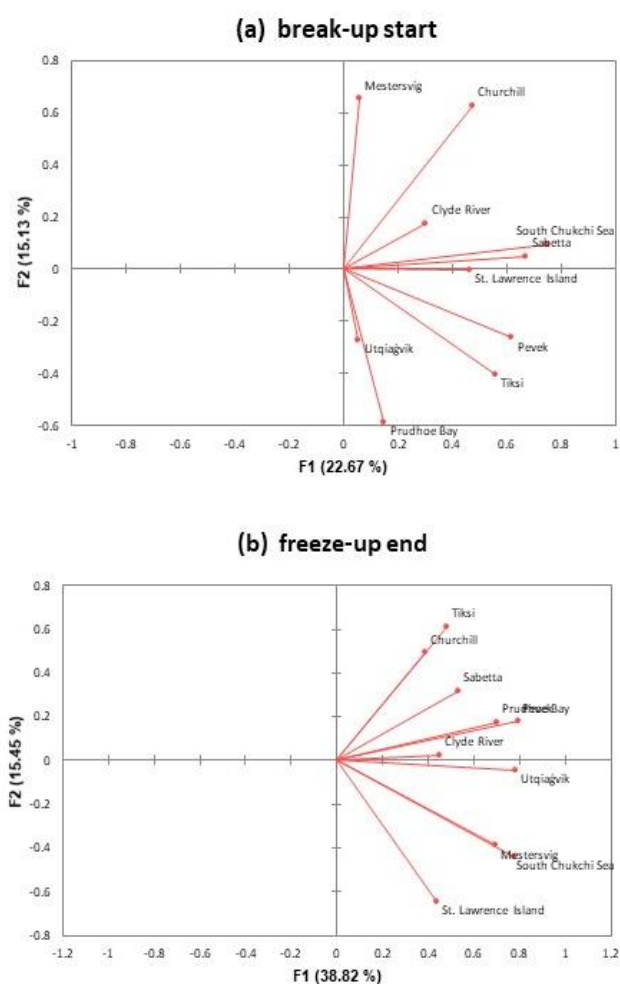
365 In order to synthesize the information provided by the local indicators, we applied a factor
366 analysis to each of the four local indicators described in Section 2. For the local indicators,
367 each matrix was 10 (locations) x 40 (years). For comparison, we also applied the factor
368 analysis to the corresponding regional sea ice areas from the MASIE database (National Snow
369 and Ice Data Center dataset G02135_v3.0-4). Because the Chukchi Sea is the MASIE region
370 for two of the local indicators (South Chukchi and Utqiagvik), the data matrix for the MASIE
371 regional factor analysis contained 9 (regions) x 40 (years) entries. We performed the MASIE
372 factors separately for middle months of the break-up and freeze-up seasons (June and
373 November, respectively).

374 In all cases, the first factor contains loadings of the same sign for all locations/regions and is
375 essentially a depiction of the temporal trends, which account for substantial percentages of the
376 variance. The second factor consists of loadings of both signs, corresponding to positive
377 departures from the mean at some locations negative departures at others. Figure 12 illustrates
378 this behavior for (a) the break-up start dates and (b) the freeze-up end dates. While every one
379 of the ten locations has a positive loading in Factor 1, the mixed signs of the Factor 2 loadings
380 point to a regional clustering of the dates. For example, Figure 12a shows that the northern
381 coastal sites in the Pacific hemisphere (Prudhoe Bay, Utqiagvik, Tiksi, Pevek) have a
382 component of break-up start date variability that is out of phase with the locations in the
383 western Atlantic/eastern Canada sector (Mestersvig, Churchill, Clyde River).

384 The interpretation of Factor 1 as a trend mode is supported by Figure 13, which shows the
385 time series of the scores of Factor 1 for (a) the break-up start date and (b) freeze-up end dates.
386 The trends towards an earlier start of break-up and a later end of freeze-up are clearly evident.
387 Figure 12 also illustrates the tendency for occasional “outlier” years to be followed by a



388 recovery in the following year. These plots and those for the other local indicators show that
389 these extreme excursions and recoveries are superimposed on the strong underlying trends,
390 resulting in new extremes when the sign of an extreme year is the same as the sign of the
391 underlying trend.

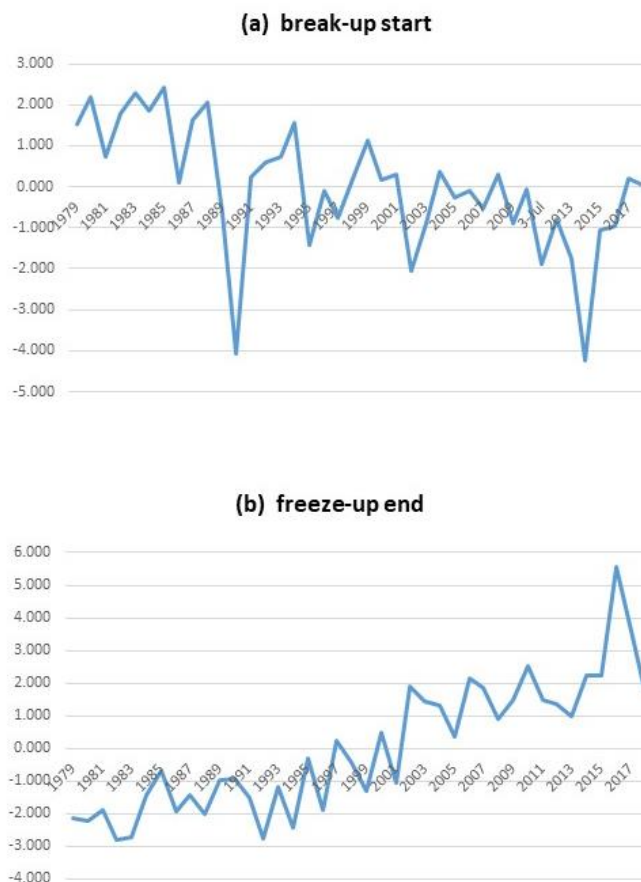


392

393 Figure 12. Loadings for Factor 1 (x-axis) and Factor 2 (y-axis) for (a) the start of break-up and (b)
394 the end of freeze-up at the ten local coastal sites. Labels on vectors denote locations.



395



396

397 Figure 13. Scores (time series) for Factor 1 of (a) the start of break-up and (b) the end of
398 freeze-up at the ten local coastal sites.

399

400 Table 3 shows that the first two factors explained more than half the variance for all local and
401 MASIE indicators except the local break-up start date. The break-up start date is notable for
402 the small percentages of variance explained by the first two factors. The implication is that



403 local conditions play a relatively greater role in the timing of the start of break-up. These local
404 factors can include landfast ice, inflow of water and heat from the adjacent land areas
405 (including rivers), and possibly other effects related to local ocean currents or local weather
406 conditions. The freeze-up start date has the most spatial coherence in the trend mode (55.7%
407 of the explained variance). However, as shown by the last two lines of Table 3, the MASIE
408 regional ice areas have even greater percentages of variance explained by the first two factors.
409 In both the break-up and freeze-up seasons (June and November), the first two factors explain
410 more than 60% of the variance (vs. 37.8%-55.7% for the local indicators). These differences
411 again point to the importance of local conditions relative to the broader underlying trend in ice
412 coverage, as Factor 1 (the trend) accounts for most of the differences between the local and
413 regional results in Table 3.

414

415 Table 3. Percentages of variance explained by Factors 1 and 2. Numbers in parentheses are
416 the contributions of the individual factors (Factor 1 + Factor 2).

417

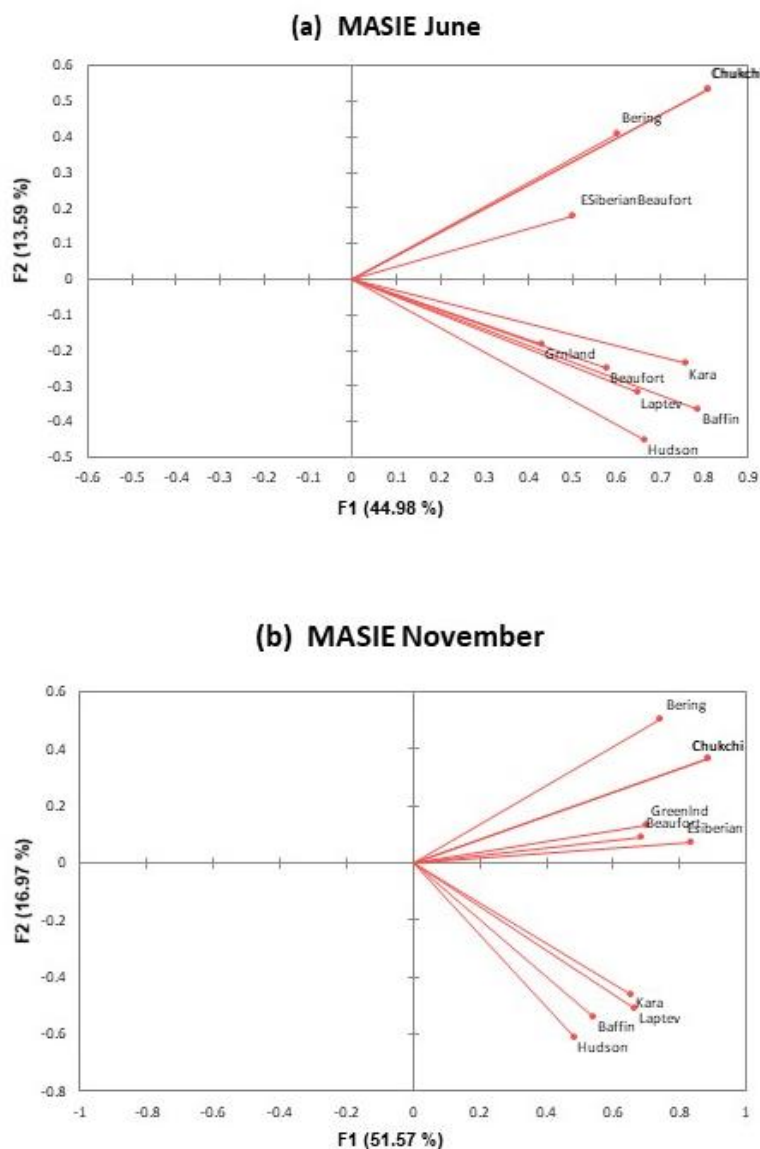
418	Break-up start	37.8%	(22.7% + 15.1%)
419	Break-up end	50.9%	(37.6% + 13.3%)
420	Freeze-up start	55.7%	(40.1% + 15.6%)
421	Freeze-up end	54.3%	(38.8% + 15.5%)
422			
423	MASIE ice areas: June	60.9%	(47.1% + 13.8%)
424	MASIE ice areas: November	64.1%	(48.7% + 15.4%)

425



426

427 Finally, Figure 14 illustrates the tendency for tighter clustering in the regional indicators. For
428 both the June and December results, the clustering in Figure 14 is clearly more distinct than in
429 Figure 12, which is the corresponding figure for the local indicators. The clustering in Figure
430 14 is geographically coherent, e.g., the Pacific sector sites (Bering, Chukchi, East Siberian)
431 are in a distinct cluster for the June (break-up), while subclusters for November include the
432 Hudson and Baffin regions, the Kara and Laptev regions, and the Bering and Chukchi regions.
433 The results imply that underlying trends and spatially coherent patterns of forcing will be
434 more useful in explaining – and ultimately predicting – variations of regional sea ice cover.
435 However, diagnosis and prediction of local indicators will require a greater reliance on
436 additional information (local geography and local knowledge, including information from
437 residents and other stakeholders who have had experience with break-up and freeze-up of sea
438 ice in the immediate area.



439

440 Figure 14. Loadings for Factor 1 (x-axis) and Factor 2 (y-axis) for the MASIE regional ice
441 areas of (a) June and (b) November. Labels on vectors denote MASIE regions.

442



443 **4. Conclusion**

444 This study has utilized sea ice indicators based on local ice climatologies informed by
445 community ice use (Johnson and Eicken, 2016; Eicken et al., 2014) rather than prescribed
446 “universal” thresholds of ice concentration (e.g., 15%, 80%) used in other recent studies of
447 sea ice break-up and freeze-up. Both types of indicators show similar trends and associated
448 interannual variations, but the more locally-tailored indicators generally show earlier break-up
449 and, in many instances, later freeze-up. The primary objective of this study was to use the
450 locally-based indicators to construct indicators of break-up and freeze-up at near-coastal
451 locations in which sea ice has high stakeholder relevance. A set of ten coastal locations
452 distributed around the Arctic were selected for this purpose.

453 The trends and interannual variations of the local indicators of break-up and freeze-up at the
454 ten nearshore are similar to the trends and variations of corresponding indicators for broader
455 offshore regions, but the site-specific indicators often differ from the regional indicators by
456 several days to several weeks. Relative to indicators for broader adjacent seas, the coastal
457 indicators show later break-up at sites known to have extensive landfast ice, whose break-up
458 typically lags retreat of the adjacent, thinner drifting ice. The coastal indicators also show an
459 earlier freeze-up at some sites in comparison with freeze-up for broader offshore regions,
460 likely tied to earlier freezing of shallow water regions and areas affected by freshwater input
461 from nearby streams and rivers. However, the trends towards earlier break-up and later freeze-
462 up are unmistakable over the post-1979 period at nearly all the coastal sites and their
463 corresponding regional seas.

464 The differences between the coastal and offshore regional indicators matter greatly to local
465 users whose harvesting of coastal resources and Indigenous culture are closely tied to the



466 timing of key events in the seasonal ice cycle (Huntington et al., 2021; Eicken et al., 2014).
467 These differences also matter from the perspective of maritime activities, where access to
468 coastal locations for destination traffic is a key factor (Brigham, 2017). These offsets vary
469 considerably by region. In light of these findings, we view locally as well as regionally
470 defined measures of sea-ice break-up and freeze-up as a key set of indicators linking pan-
471 Arctic or global indicators such as sea-ice extent or volume to local and regional uses of sea
472 ice, with the potential to inform community-scale adaptation and response.

473

474 **Acknowledgments**

475 This work was supported by the Climate Program Office of the National Oceanic and
476 Atmospheric Administration through Grant NA17OAR431060.

477

478 **Data Availability**

479 The daily grids of passive-microwave-derived sea ice concentrations are available from the
480 National Snow and Ice Data Center as dataset NSIDC-0051, available at
481 <https://nsidc.org/data/nsidc-0051>. Lists of the indicator dates for the coastal sites and the
482 MASIE regions are available from the author on request.

483

484 **Author contributions**

485 JEW served the principal investigator for the study, led the drafting of the manuscript, and
486 performed the factor analysis described in Section 4. HE supervised the implementation of



487 the revised indicators for the coastal sites and the MASIE regions, and drafted parts of the
488 text. KR performed the indicator calculations, produced Figures 1-11, and assisted in the
489 preparation of the manuscript. MJ designed the original indicators, participated in the
490 modification of the indicators, and contributed to the revision of the manuscript.

491

492 **Competing interests**

493 The authors declare that they have no conflict of interest

494

495

496 **References**

- 497 AMAP: Snow, water, ice and permafrost in the Arctic (SWIPA), Arctic Monitoring and
498 Assessment Programme (AMAP), Oslo, Norway, 2017.
- 499
500 Bliss, A.C., and Anderson, M.R.: Arctic sea ice melt onset and timing from passive
501 microwave- and surface air temperature-based methods, *J. Geophys. Res.*, 123, 9063-9080,
502 <https://doi.org/10.1029/2018JD028676>, 2018.
- 503
504 Bliss, A.C., Steele, M., Peng, G., Meier, W.M., and Dickinson, S: Regional variability of
505 Arctic sea ice seasonal climate change indicators from a passive microwave climate data
506 record, *Environ. Res. Lett.*, 14, 045003, <https://doi.org/10.1088/1748-9326/aafb84>, 2019.
- 507
508 Box, J.E., and 19 coauthors: Key indicators of Arctic climate change: 1971–2017, *Environ.*
509 *Res. Lett.*, 14(4), p.045010, <https://doi.org/10.1088/1748-9326/aafc1b>, 2019.
- 510
511 Brigham, L.W.: The changing maritime Arctic and new marine operations. In: Beckman, R.
512 C., Henriksen, T., Dalaker Kraabel, K., Molenaar, E. J., and Roach, J. A. (eds.): *Governance*
513 *of Arctic shipping* (pp. 1-23). Brill Nijhoff, 2017.
- 514
515 Cavalieri, D. J., Gloersen, P., and Campbell, W. J.: Determination of Sea Ice Parameters with
516 the NIMBUS-7 SMMR, *J. Geophys. Res.*, 89(D4): 5355-5369,
517 <https://doi.org/10.1029/JD089iD04p05355>, 1984.
- 518
519 Comiso, J. C: Characteristics of Arctic Winter Sea Ice from Satellite Multispectral
520 Microwave Observations, *J. Geophys. Res.*, 91(C1), 5C0766, 975-994, 1986
- 521
522 Dammann, D. O., Eicken, H., Mahoney, A. R., Meyer, F. J. and Betcher, S: Assessing sea ice
523 trafficability in a changing Arctic. *Arctic*, 71(1), 59-75, <https://doi.org/10.14430/arctic4701>,
524 [2018](https://doi.org/10.14430/arctic4701).



- 525
526 Deser, C., Walsh, J. E., and Timlin, M. S.: Arctic sea ice variability in the context of recent
527 atmospheric circulation trends, *J. Climate*, 13, 617-633, DOI: [https://doi.org/10.1175/1520-0442\(2000\)013<0617:ASIVIT>2.0.CO;2](https://doi.org/10.1175/1520-0442(2000)013<0617:ASIVIT>2.0.CO;2), 2000.
- 528
529
530 Eicken, H., Kaufman, M., Krupnik, I., Pulsifer, P., Apangalook, L., Apangalook, P., Weyapuk
531 Jr, W., and Leavitt, J.: A framework and database for community sea ice observations in a
532 changing Arctic: An Alaskan prototype for multiple users, *Polar Geogr.*, 37(1), 5-27,
533 <http://dx.doi.org/10.1080/1088937X.2013.873090>, 2014.
- 534
535 Fang, A., and Wallace, J. M.: Arctic sea ice variability on a timescale of weeks in relation to
536 atmospheric forcing, *J. Climate*, 7, 1897-1914, [https://doi.org/10.1175/1520-0442\(1994\)007<1897:ASIVOA>2.0.CO;2](https://doi.org/10.1175/1520-0442(1994)007<1897:ASIVOA>2.0.CO;2), 1994. .
- 537
538
539 Fu, D., Liu, B., Yu, G., Huang, H., and Qu, L: Multiscale variations in Arctic sea ice motion
540 and links to atmospheric and oceanic conditions, *The Cryosphere*, 15, 3797-3811,
541 <https://doi.org/10.5194/tc-15-3797-2021>, 2021.
- 542
543 Hosekova, L., Eidam, E., Panteleev, G., Rainville, L., Rogers, W. E., and Thomson, J.:
544 Landfast ice and coastal wave exposure in northern Alaska. *Geophys. Res. Lett.*, 48(22),
545 p.e2021GL095103, <https://doi.org/10.1029/2021GL095103>, 2021.
- 546
547 Huntington, H. P., Raymond-Yakoubian, J., Noongwook, G., Naylor, N., Harris, C.,
548 Harcharek, Q. and Adams, B.: “We never get stuck:” A collaborative analysis of change and
549 coastal community subsistence practices in the northern Bering and Chukchi Seas,
550 *Alaska, Arctic*, 74(2), 113-126, 2021.
- 551
552 IPCC: Climate Change 2021: The Physical Science Basis. Contribution of Working Group I
553 to the Sixth Assessment Report of the Intergovernmental Panel on Climate Change [Masson-
554 Delmotte, V., Zhai, P., Pirani, A., Connors, S. L., Péan, C., Berger, S., Caud, N., Chen, Y.,
555 Goldfarb, L., Gomis, M. I., Huang, M., Leitzell, K. Lonnoy, E., Matthews, J. B. R., Maycock,
556 T. K., Waterfield, Y., Yelekçi, O., Yu, R., and Zho, B. (eds.)]. Intergovernmental Panel on
557 Climate Change, Cambridge University Press.
558 [https://www.bing.com/search?FORM=AFSCVO&PC=AFSC&q=IPCC+AR6+Working+Gro](https://www.bing.com/search?FORM=AFSCVO&PC=AFSC&q=IPCC+AR6+Working+Group+1+report)
559 [up+1+report](https://www.bing.com/search?FORM=AFSCVO&PC=AFSC&q=IPCC+AR6+Working+Group+1+report), 2022.
- 560
561 Johnson, M., and Eicken, H.: Estimating Arctic sea-ice freeze-up and break-up from the
562 satellite record: A comparison of different approaches in the Chukchi and Beaufort Seas,
563 *Elements: Science of the Anthropocene*, 4, 000124, doi:10.12952/journal.elementa.000124,
564 2016.
- 565
566 Markus, T., Stroeve J. C., and Miller, J: Recent changes in Arctic sea ice melt onset, freezeuo
567 and melt season length, *J. Geophys. Res. (Oceans)*, 114, 1-14,
568 <https://doi.org/10.1029/2009JC005436>, 2009.
- 569



- 570 Meier, W., Fetterer, F., Savoie, M., Mallory, S. Duerr, R., and Stroeve, J.: NOAA/NSIDC
571 Climate Data Record of Passive Microwave Sea Ice Concentration, Version 3 (Boulder,
572 Colorado USA; National Snow and Ice Data Center), <https://doi.org/10.7265/N59P2ZTG>,
573 [Accessed 16 January 2022], 2017
574
- 575 Peng, G., Steele, M., Bliss, A. C. Meier, W. N., and Dickinson, S: Temporal means and
576 variability of Arctic sea ice melt and freeze season climate indicators using a satellite climate
577 data record, *Remote Sensing*, 10, 1328, <https://doi.org/10.3390/rs10091328>, 2018
578
- 579 Smith, A., and Jahn, A.: Definition differences and internal variability affect the simulated
580 Arctic sea ice melt season, *The Cryosphere*, 12, 1-20, <https://doi.org/10.5194/tc-13-1-2019>,
581 2019.
582
- 583 Walsh, J. E., and Johnson, C. M.: Interannual atmospheric variability and associated
584 fluctuations in Arctic sea ice extent, *J. Geophys. Res.*, 84, 6915–6928,
585 <https://doi.org/10.1029/JC084iC11p06915>, 1979.
586
587
588